Lessons from a gene knockout mouse model: no phenotypes induced by deletion of the TPR4 domain of Ttc22

Running title: *Ttc22* exon 2&3-deleted mouse

Jiaoyang Liu, Liankun Gu, Abin You, Hongfan Yuan, Jing Zhou, Wei Tian*, Dajun Deng*

Key Laboratory of Carcinogenesis and Translational Research (MOE/Beijing), Division of Etiology, Peking University Cancer Hospital and Institute, Beijing, 100142, China

Corresponding authors: Wei Tian or Dajun Deng, Key Laboratory of Carcinogenesis and Translational Research (MOE/Beijing), Division of Etiology, Peking University Cancer Hospital and Institute, Fu-Cheng-Lu #52, Haidian District, Beijing, 100142, China, Phone:+8610-88196752 (E-mail: tianwei@bjmu.edu.cn or dengdajun@bjmu.edu.cn; ORCID: 0000-0003-2853-7056 or 0000-0001-5161-5943)

Highlights

- Knockout of *Ttc22* exons 2 and 3 does not affect the development of C57BL mice.
- *Ttc22* knockout does not affect the induction of mouse colon cancer by AOM/DSS.
- Loss of the *Ttc22* exons 2 and 3 cannot disrupt the functions of TTC22.

Email address

Jiaoyang Liu, pocky1995@126.com
Liankun Gu, gulkun@163.com
Abin You, youabin115@126.com
Hongfan Yuan, yuanhongfan@scszlyy.org.cn
Jing Zhou, jane72@163.com
Wei Tian, tianwei@bjmu.edu.cn
Dajun Deng, dengdajun@bjmu.edu.cn

ABSTRACT

The *TTC22* gene encodes a protein containing seven tetratricopeptide repeats (TPRs), which mediate protein−protein interactions as chaperones. We previously reported that the level of *TTC22* transcript variant 1 (*TTC22v1*) was downregulated in human colon adenocarcinoma (COAD) and that TTC22 upregulated m6A-mediated *WTAP* and *SNAI1* expression via the TTC22−RPL4 interaction and subsequently promoted COAD metastasis. Thus, a commercially available C57BL/6N mouse model in which the *Ttc22* exon 2&3 encoding the TPR4 (equal to the human TTC22 TPR3) domain was knocked out via CRISPR-Cas9 was used to evaluate the contribution of *Ttc22* to the development of mice and COAD. Unfortunately, the long-term observation results demonstrated that *Ttc22* knockout (KO, including *Ttc22*$^{-/+}$ or *Ttc22*$^{-/-}$) did not affect the body weight, development, fertility, or spontaneous tumor incidence of male or female mice. No differences in the incidence of AOM/DSS-induced COAD were observed between these mouse groups, although *Ttc22* exon 2&3 deletion partially resulted in the upregulation of adaptive response genes in the colon mucosa. Further study revealed that TPR4 deletion did not disrupt the effect of TTC22 on WTAP upregulation. Consistently, TPR4 deletion did not affect the abundance of total RNA m6A in the colon tissues of the mice, suggesting that the TPR4-deleted Ttc22 mutant remains functional. In conclusion, the TPR4 domain is not essential for the Ttc22 protein. Loss of Ttc22 TPR4 caused no observable changes in the development of C57BL mice or their susceptibility to treatment with the chemical carcinogen AOM/DSS. Whether an essential sequence for a target gene is knocked out should be carefully evaluated before a gene knockout model is employed in formal experiments.

Keywords: Ttc22; TPR4 deletion; C57BL/6N mouse; development; colon cancer; AOM/DSS

44 **INTRODUCTION**

45 The human TTC22 protein contains seven tetratricopeptide repeats (TPRs), which mediate protein−
46 protein interactions and are involved in multiple biological processes, including the movements of cilia
47 and flagella and the migration of human cells [1-5]. A pilot study reported that the *TTC22* gene was among
48 the top ten downregulated genes in the fetuses of obese women compared with lean women in the
49 second trimester and that low *TTC22* expression in mothers may be related to fetal neurodevelopment
50 and metabolism [6]. Differentially methylated regions of the *TTC22* gene are associated with hand grip
51 strength [7]. DNA sequencing and transcriptome data analyses in 3,203 subjects suggested that
52 low-frequency variants of *TTC22* were associated with LDL cholesterol [8]. These phenomena imply that
53 TTC22 may be involved in physiological metabolism. However, the causality between TTC22 alterations
54 and metabolism is not known.

55 The *TTC22* gene is comprehensively expressed in epithelial cells in the normal gut mucosa at the
56 middle level and is extensively downregulated in gastrointestinal cancer tissues, according to the
57 databases from the Human Protein Atlas and The Cancer Genome Atlas (TCGA) [9,10]. We initially
58 reported that *TTC22* variant 1 (*TTC22v1*) mRNA is targeted by *miR663a*, an anti-inflammatory miRNA in
59 the colon [11]. The level of *TTC22v1* mRNA is significantly lower in human colon adenocarcinoma (COAD)
60 than in paired normal tissue samples, and high *TTC22* expression increases the risk of colon cancer
61 metastasis. Our further study revealed that TTC22 increased m6A-mediated *WTAP* and *SNAI1* expression
62 via TTC22-RPL4 binding and subsequently promoted COAD metastasis *in vitro* and *in vivo* [12], suggesting
63 a potential role for TTC22 in the development and progression of COAD.

64 Therefore, we further studied the effects of Ttc22 on the development of mice and their
65 susceptibility to the chemical carcinogen AOM/DSS via a genetically established and commercially
66 available C57BL gene knockout mouse model in which *Ttc22* exons 2 and 3, which encode the TPR4
67 domain of the mouse Ttc22 protein, were knocked out via CRISPR−Cas9. Unexpectedly, no differences in
68 the development, growth, fertility, or AOM/DSS susceptibility of the mice were induced by TPR4 deletion.
69 Our further study results indicated that the TPR3 domain (equal to mouse TTC22 TPR4) is not essential for
70 TTC22 to upregulate WTAP and related m6A modifications. Although commercially available gene
71 knockout models are useful for scientists in molecular biology and pathogenesis, whether such models are
72 eligible for use should be carefully evaluated before they are formally used in experiments.

MATERIALS AND METHODS

Ttc22 exon 2&3 knockout mouse model

Genetically established *Ttc22* knockout (Ttc22-KO) C57BL/6N mice (strain S-KO-06335) were purchased from Cyagen (Cyagen Bio. Co., Guangzhou, China). Ttc22 knockout mice were obtained via high-throughput electroporation of fertilized eggs. The CRISPR-Cas9 system and two gRNAs (gRNA#1: 5'-ggaaagugggcauaacgccuggg-3' and gRNA#2: 5'-uuccagagagauagcgaccgagg-3') targeted to *Ttc22* introns 1&3 were used to delete a 1610 bp fragment including *Ttc22* exons 2&3 encoding the Ttc22 TPR4 domain (Figure 1A). After sexual maturity, sperm were collected for cryopreservation. Through hybridization with female wild-type C57BL/6N mice, first-generation Ttc22$^{+/-}$ mice were obtained and used to generate male and female mice with different *Ttc22* genotypes (including Ttc22$^{+/+}$, Ttc22$^{+/-}$, and Ttc22$^{-/-}$), as determined by PCR sequencing via the tail DNA template and two forward primers (OuterF: 5'-tcacaacctactcaagatccagc-3' and InnerF: 5'-caactgtagggtatagcagtccc-3') and one common reverse primer (5'-ttattgcctccttggtgagttg-3'). A mouse tissue direct PCR kit (YEASEN, Shanghai, China) was used to amplify *Ttc22.* Both male and female *Ttc22*$^{+/+}$ and *Ttc22*$^{-/-}$ mice were maintained as seed mice in an animal facility under SPF conditions at the Peking University Cancer Hospital & Institute. The seed mice were hybridized to generate experimental mouse stocks with different *Ttc22* genotypes. The body weight of each mouse was measured once a week from 4–31 weeks of age. The animal experiments were approved by the Biomedical Ethical Committee of Peking University Cancer Hospital & Institute.

High-fat diet experiment

Four-week-old female C57BL/6N mice were fed a high-fat diet (4.73 kcal/g，H10045, Huafukang Bio. Co., Beijing, China). Additionally, a control group of four-week-old female mice was fed a regular diet. The mice were housed in a temperature-controlled room with a 12-hr light/dark cycle. All the mice had free access to food and water [13].

Fertility test

Mating tests were carried out with 6–8-week-old mice. One male Ttc22$^{+/+}$ mouse was mated with 1 Ttc22$^{+/+}$ female mouse as the control group, and 1 male Ttc22$^{-/-}$ mouse was mated with 1 Ttc22$^{-/-}$ female mouse as the Ttc22-KO group for at least 3 months. At least three mates were included in each group. The date and number of pups were recorded at birth in each cage.

103 **Induction of COAD by AOM/DSS**

104 Five male mice aged 6–8 weeks were included in each group within the same cage. The mice in the three
105 groups, *Ttc22*$^{+/+}$, *Ttc22*$^{+/-}$, and *Ttc22*$^{-/-}$ were intraperitoneally administered 10 mg/kg b.w. azoxymethane
106 (AOM) solution (1 mg/mL, freshly prepared with saline; Cat. #A5486, Sigma − Aldrich; Merck KGaA,
107 Darmstadt, Germany) on the 1st experimental day. Beginning on the 2nd experimental day, the mice were
108 administered dextran sodium sulfate (DSS; Cat. #24867; Sigma) in the drinking water containing 2.5% DSS
109 (2.5 g/100 mL) for 7 continuous days. The mice were subsequently allowed to recover for three weeks
110 (drinking water not containing DSS). The combined AOM/DSS treatment cycle was repeated two more
111 times [14]. From the 24th to 27th experimental weeks, the mice were sacrificed, the colon was collected,
112 and the length of the colon was measured. The intestine was opened, and the colon mucosa was carefully
113 examined and photodocumented. Evidence of gross pathologic changes was recorded (e.g., ulceration).
114 Then, the colon tissues were fixed with 10% formalin, rolled Swiss, embedded in paraffin, and sectioned
115 for pathological analysis. Some of the colon tissues were snapped and frozen for RNA extraction or
116 homogenized in RIPA buffer for protein extraction. The roll was further fixed in 10% buffered formalin
117 overnight at room temperature and used to prepare tissue sections (4 µm). Pathology was performed by
118 senior pathologists.

119 **Quantitative RT−PCR (qRT−PCR)**

120 Total RNA was extracted from fresh tissue samples via TRIzol Reagent (ZYMO Research, Beijing, China)
121 according to the manufacturer's instructions within 5 min of euthanization. First-strand cDNA was
122 generated via a TransScript First-Strand cDNA Synthesis Kit (TransGen Biotech, Beijing, China). Exon−exon
123 qRT−PCR was performed via FastStart Universal SYBR Green Master Mix (Roche, Mannheim, Germany).
124 Mouse *Gapdh* mRNA (forward primer: 5'-ggttgtctcctgcgacttca-3' and reverse primer:
125 5'-tggtccagggtttcttactcc-3') was used as an internal control for *Ttc22* mRNA (forward primer:
126 5'-gatatgcgcatggcttcgac-3' and reverse primer: 5'-tgccatggtgaagtaccagc-3'). The relative *Ttc22* mRNA level
127 was calculated via the typical $2^{-\Delta\Delta CT}$ method.

128 **RNA sequencing**

129 Total RNA was extracted from the colon tissues of three male mice with different *Ttc22* genotypes via an
130 RNA extraction kit. RNA sequencing was performed by Cloud-Seq Biotech (Shanghai, China). Briefly, total
131 RNA was removed from the rRNAs with an NEBNext rRNA depletion kit (Biolabs, Inc., Massachusetts, USA),

132 which was subsequently used to construct RNA libraries via the NEBNext Ultra II directional RNA library
133 prep kit (Biolabs). Library sequencing was performed on an Illumina NovaSeq 6000 instrument with 150
134 bp paired-end reads. Paired-end reads were harvested. The high-quality clean reads were aligned to the
135 reference genome with HISAT2 software (v2.0.4), guided by the Ensembl gtf gene annotation file, and the
136 gene level FPKM was obtained as the expression profile of the mRNAs. Fold changes and p values were
137 calculated on the basis of the FPKM values, and the differentially expressed mRNAs were identified on the
138 basis of $|\log(FC)|>=1.0$, p value<= 0.05). GO and pathway enrichment analyses were performed on the
139 differentially expressed mRNAs. The raw data were deposited under the Gene Expression Omnibus
140 accession number GSE275363.

141 **m6A dot blot analysis**

142 m6A dot blot analysis was performed as we previously reported [12].

143 **Quantification of the m6A abundance via m6A-specific ELISA**

144 The total RNA m6A level was quantified with an EpiQuik m6A RNA Methylation Quantification Kit (P-9005;
145 Epigentek Group, NY, USA) according to the manufacturer's instructions [15,16].

146 **LC–MS/MS measurement of the m6A/rA ratio**

147 Liquid-MS/MS quantification of m6A was performed by Cloudseq Biotech, Inc. (Shanghai, China), as
148 described previously [12].

149 **Full-length TTC22, ΔTPR1, and ΔTPR4 expression vectors**

150 The pCMV6-Entry-Myc/Flag full-length TTC22 and ΔTPR1 expression vectors were the same as those
151 previously reported [12]. The ΔTPR3 vector not containing 190-246 aa (equal to the mouse Ttc22 TPR4
152 domain encoding sequence) was derived from the full-length TTC22 vector. These vectors were used to
153 transiently transfect human colon cancer HCT116 cells (ATCC; Manassas, VA, USA).

154 **Statistical analysis**

155 Statistical analysis was carried out via SPSS 22. 0 software (SPSS Inc., Chicago IL, USA). The data are
156 presented as the means ± SDs of at least three independent experiments or as the medians (25th–75th
157 percentiles). Statistical analysis methods included Student's t test, one-way analysis of variance (ANOVA),
158 and two-way ANOVA. The exact statistical methods are described in detail for each experiment in the

159 Results section. All tests were two-sided. A p value <0.05 was considered to indicate statistical
160 significance.

161 ## RESULTS

162 **Characterization of *Ttc22* genotypes**

163 To evaluate the effects of the *Ttc22* gene on the development of mice and COAD, a commercially available
164 heterozygous Ttc22-KO C57BL/6N mouse model was used to generate mice with various *Ttc22* genotypes,
165 including homozygous and heterozygous Ttc22-KO ($Ttc22^{-/-}$ and $Ttc22^{+/-}$) and its wild-type control ($Ttc22^{+/+}$)
166 via serial hybridization, as described in the Methods section. The sequencing results indicated that a 1610
167 bp fragment, including *Ttc22* exons 2 and 3, which encode the Ttc22 TPR4 domain (58 aa), was deleted via
168 CRISPR-Cas9 and two gRNAs (Figure 1A and 1B). RNA sequencing confirmed the sequencing results (Figure
169 1C).

170 **No morphologic alterations in heterozygous and homozygous Ttc22-KO mice**

171 Compared with wild-type C57BL/6N mice, those with different *Ttc22* knockout states did not differ in
172 development, growth, appearance (Figure 2), body weight (Figure 3A and 3B), or fertility (Figure 4).

173 Considering that *TTC22* is mostly downregulated in the fetuses of obese women and that
174 low-frequency variants of TTC22 are associated with LDL cholesterol in the human body [1,3], we further
175 compared the body weights of female *Ttc22* mice fed a high-fat diet. However, no differences in the body
176 weights of C57BL/6N mice in different *Ttc22* genotype groups were observed (Figure 3C).

177 No spontaneous tumors were observed in these mice up to 40 weeks of age. As expected,
178 spontaneous tumors, including sebaceous carcinoma and basal carcinoma, occurred in some old mice.
179 However, no differences in the incidence of spontaneous tumors were detected between these *Ttc22*
180 genotype groups (Table S1).

181 **No differences in AOM/DSS-induced COAD between $Ttc22^{+/+}$, $Ttc22^{+/-}$, and $Ttc22^{-/-}$ mice**

182 Because *TTC22* is involved in COAD metastasis [5,6], we wondered whether Ttc22-KO might affect the
183 biological processes of the colon and the development of COAD. We performed RNA sequencing on total
184 RNA extracted from the colons of 58-week-old male mice. The GO and pathway analysis results revealed
185 that Ttc22-KO mainly upregulated genes related to microorganism infection (Figure 5), supporting the
186 hypothesis that Ttc22 may contribute to host defensive responses against infection.

187 We further studied whether Ttc22-KO affects the development of colorectal tumors induced by three
188 cycles of AOM/DSS treatment in male mice. By the end of the 24th or 27th experimental week,
189 well-differentiated or moderately differentiated adenocarcinomas were induced in the colons of all
190 AOM/DSS-treated mice but not in those of the 0.9% NaCl control mice (Figure 6). No differences in the
191 incidence or severity of colorectal tumors were observed between these mice with different *Ttc22*
192 genotypes.

193 **The TPR4 domain is not essential for TTC22 function**

194 We recently reported that the TPR1 domain, but not the TPR3 or TPR4 domain, is essential for the
195 TTC22-RPL4 interaction [12]. However, whether the TTC22 TPR3 or TPR4 domain contributes to WTAP
196 expression and total RNA m6A levels has not been previously reported. We studied the effect of the loss
197 of the human TTC22 TPR3 (equal to the mouse Ttc22 TPR4) domain on WTAP expression in human colon
198 cancer HCT116 cells (Figure 7A). As we previously reported [12], deletion of the TPR1 domain (ΔTPR1)
199 abolished the ability of TTC22 to increase WTAP and RNA m6A abundance. However, deletion of the TPR3
200 domain (ΔTPR3) did not abolish the ability of TTC22 to regulate WTAP and RNA m6A modification (Figure
201 7B and 7C). The results of the ELISA confirmed the results of the dot blot analysis (Figure 7D). These
202 findings suggest that deletion of the human TTC22 TPR3 (or mouse Ttc22 TPR4) domain did not disrupt
203 the upregulation of WTAP expression and m6A modification by TTC22. Consistently, the results of liquid
204 chromatography−mass/mass (LC−MS/MS) analysis revealed no difference in total RNA m6A abundance in
205 colon tissue samples from the three groups of mice (Figure 7E).

206 ## DISCUSSION

207 Considering that *TTC22* mediates human COAD metastasis [11,12], we studied the influence of *Ttc22*
208 knockout on the development of COAD in C57BL/6N mice. Unfortunately, no significant differences in the
209 development or fertility of mice and AOM/DSS-induced COAD were observed between wild-type and
210 Ttc22-KO C57BL/6N mice, probably because deletion of the Ttc22 TPR4 domain could not disrupt *Ttc22*
211 functions in the commercially available gene knockout model.

212 The AOM/DSS-mediated COAD model is an inflammation-related cancer model. The similar
213 prevalence of COAD induced by AOM/DSS in all of these mice suggests that the doses of AOM and DSS
214 administered were too high to display the effects of Ttc22-KO on colon tumorigenesis or that the loss of
215 the Ttc22 TPR4 (equal to the human TTC22 TPR3) domain does not disrupt the biological functions of the

216 Ttc22 protein in mice. Although we cannot exclude the possibility that biological inactivation of *Ttc22* may
217 not induce phenotypic alterations, our findings that deletion of human TTC22 TPR3 (ΔTPR3) does not
218 abolish *WTAP* upregulation via TTC22 and that there are no differences in total RNA m6A levels between
219 Ttc22-KO and Ttc22-WT mice strongly suggest that the commercial Ttc22-KO model is not an eligible
220 model that leads to the above negative observations.

221 Gene knockout animal models are important research tools for validating the biological functions of
222 target genes. The emergence of commercially available gene knockout mouse models has greatly
223 promoted research progress in biology, pathogenesis, and drug development. However, most commercial
224 gene knockout mouse models are not stringently created on the basis of biological inactivation of the
225 target genes by CRISPR-Cas9. Instead, they are often randomly created using many guide RNAs (gRNAs)
226 targeted to various genes in the whole genome. Because of the high labor and financial costs of
227 establishing a target DNA sequence-specific knockout mouse model, biological and medical researchers
228 like to use commercially available gene knockout mouse models directly. Our experience indicates that
229 careful evaluation of the eligibility of such a mouse model is essential before the model is used in formal
230 experiments.

231 In conclusion, we found that deletion of the Ttc22 TPR4 domain does not disrupt Ttc22 functions and
232 thus does not induce abnormal phenotypes in mice, including development, growth, or COAD induction
233 by AOM/DSS. Only eligible gene knockout mouse models should be used in formal experiments.

234 Abbreviations

235 COAD, colon adenocarcinoma

236 Ttc22, tetratricopeptide repeat domain 22

237 AOM, azoxymethane

238 DSS, dextran sodium sulfate

239 **Funding** This work was supported by grants from the Beijing Hospital Authority Mission Plan
240 (SML20191101) to DD and from the Science Foundation of Peking University Cancer Hospital (grant
241 #2022-8) to TW.

242 Author contributions

243 Conceptualization: DJD, WT, ABY; Funding acquisition: DJD; Investigation: JYL, WT, LKG, ABY, HFY, JZ;

Methodology: WT; Project administration: DJD and WT; Visualization: DJD and WT; Writing – original draft: JYL, WT, and DJD; Writing – review & editing: all authors

Competing interest

The authors declare that they have no competing interests.

Acknowledgments

We acknowledge the support from Beijing Hospital Authority and Peking University Cancer Hospital for this project. We also extend our gratitude to staff from the laboratory animal center at Peking University Cancer Hospital for their care and maintenance of the animals.

REFERENCE

1. D'Andrea, L. TPR proteins: the versatile helix. *Trends in Biochemical Sciences*, 2003. 28(12): 655-662.
2. Hesketh SJ, Mukhopadhyay AG, Nakamura D, Toropova K, Roberts AJ. IFT-A structure reveals carriages for membrane protein transport into cilia. Cell, 2022. 185(26): 4971-4985.e16.
3. Shamoto N, Narita K, Kubo T, Oda T, Takeda S. CFAP70 Is a Novel Axoneme-Binding Protein That Localizes at the Base of the Outer Dynein Arm and Regulates Ciliary Motility. Cells, 2018. 7(9): p. 124.
4. Vomastek T, Iwanicki MP, Burack WR, Tiwari D, Kumar D, Parsons JT, Weber MJ, Nandicoori VK. Extracellular signal-regulated kinase 2 (ERK2) phosphorylation sites and docking domain on the nuclear pore complex protein Tpr cooperatively regulate ERK2-Tpr interaction. Mol Cell Biol. 2008 Nov;28(22):6954-66.
5. McCloskey A, Ibarra A, Hetzer MW. Tpr regulates the total number of nuclear pore complexes per cell nucleus. Genes Dev. 2018 Oct 1;32(19-20):1321-1331.
6. Edlow AG, Vora NL, Hui L, Wick HC, Cowan JM, Bianchi DW. Maternal obesity affects fetal neurodevelopmental and metabolic gene expression: a pilot study. PLoS One, 2014 Feb 18;9(2):e88661.
7. Soerensen, M. *et al.* Epigenome-wide exploratory study of monozygotic twins suggests differentially methylated regions to associate with hand grip strength. Biogerontology, 2019;20, 627-647.
8. Yang T, Wu C, Wei P, Pan W. Integrating DNA sequencing and transcriptomic data for association analyses of low-frequency variants and lipid traits. Hum Mol Genet. 2020 Feb 1;29(3):515-526.
9. Uhlén M, Fagerberg L, Hallström BM, Lindskog C, Oksvold P, Mardinoglu A, Sivertsson Å, Kampf C,

272 Sjöstedt E, Asplund A, et al: Proteomics. Tissue-based map of the human proteome. Science, 2015,
273 347:1260419.
274 10. Cerami E, et al. The cBio cancer genomics portal: an open platform for exploring multidimensional
275 cancer genomics data. Cancer Discov. 2012, 2:401-404.
276 11. Tian W, Du Y, Ma Y, Zhang B, Gu L, Zhou J, Deng D. miR663a‐TTC22V1 axis inhibits colon cancer
277 metastasis. Oncol Rep. 2019 Mar;41(3):1718-1728.
278 12. You A, Tian W, Yuan H, Gu L, Zhou J, Deng D. TTC22 promotes m6A-mediated WTAP expression and
279 colon cancer metastasis in an RPL4 binding-dependent pattern. Oncogene, 2022
280 Aug;41(32):3925-3938.
281 13. Nakamura Y, Natsume M, Yasuda A, Ishizaka M, Kawahat K, Koga J. Fructooligosaccharides suppress
282 high-fat diet-induced fat accumulation in C57BL/6J mice. Biofactors, 2017. 43(2): p. 145-151.
283 14. Angelou A, Andreatos N, Antoniou E, Zacharioudaki A, Theodoropoulos G, Damaskos C, Garmpis N,
284 Yuan C, Xiao W, Theocharis S, Zografos G, Papalois A, Margonis GA. A Novel Modification of the
285 AOM/DSS Model for Inducing Intestinal Adenomas in Mice. Anticancer Res. 2018
286 Jun;38(6):3467-3470.
287 15. Xu Y, Zhou J, Li L, et al. FTO-mediated autophagy promotes progression of clear cell renal cell
288 carcinoma via regulating SIK2 mRNA stability. Int J Biol Sci. 2022; 18(15):5943-5962.
289 16. Ren QW, Xiang MY, Qiao JL, Liu ZJ, Zhang G, Gu LK, Zhou J, Tian W, Deng DJ. TTC7B triggers the
290 PI4KA-AKT1-RXRA-FTO axis and inhibits colon cancer cell proliferation by increasing RNA methylation.
291 Int J Biol Sci. 2025; 21(3):1127-1143.

FIGURES AND LEGENDS

Figure 1. Characterization of the genotypes of the *Ttc22* gene in C57BL/6N mice via CRISPR-Cas9. (**A**) Locations of the deleted fragment (1610 bp), amplicons, gRNAs, and primers matched to the *Ttc22* gene. The conservation status of *Ttc22* in placental mammals, including rats, rabbits, and humans, is displayed below. (**B**) Characterization of *Ttc22* genotypes, as determined by PCR and sequencing. The wild-type *Ttc22* fragment is too long (2438 bp) to be amplified via regular PCR via the OuterF and OuterR primer sets. (**C**) IGV view of *Ttc22* transcripts in RNA samples from the colons of three male mice with different *Ttc22* genotypes, including *Ttc22* wild-type ($Ttc22^{+/+}$), heterozygously deleted ($Ttc22^{-/+}$), and homozygously deleted ($Ttc22^{-/-}$) strains, as determined by RNA sequencing. The exon 2&3 region, which is shared by both *Ttc22* variants 1 and 2 and is knocked out by CRISPR-Cas9, is highlighted by a red rectangle.

305

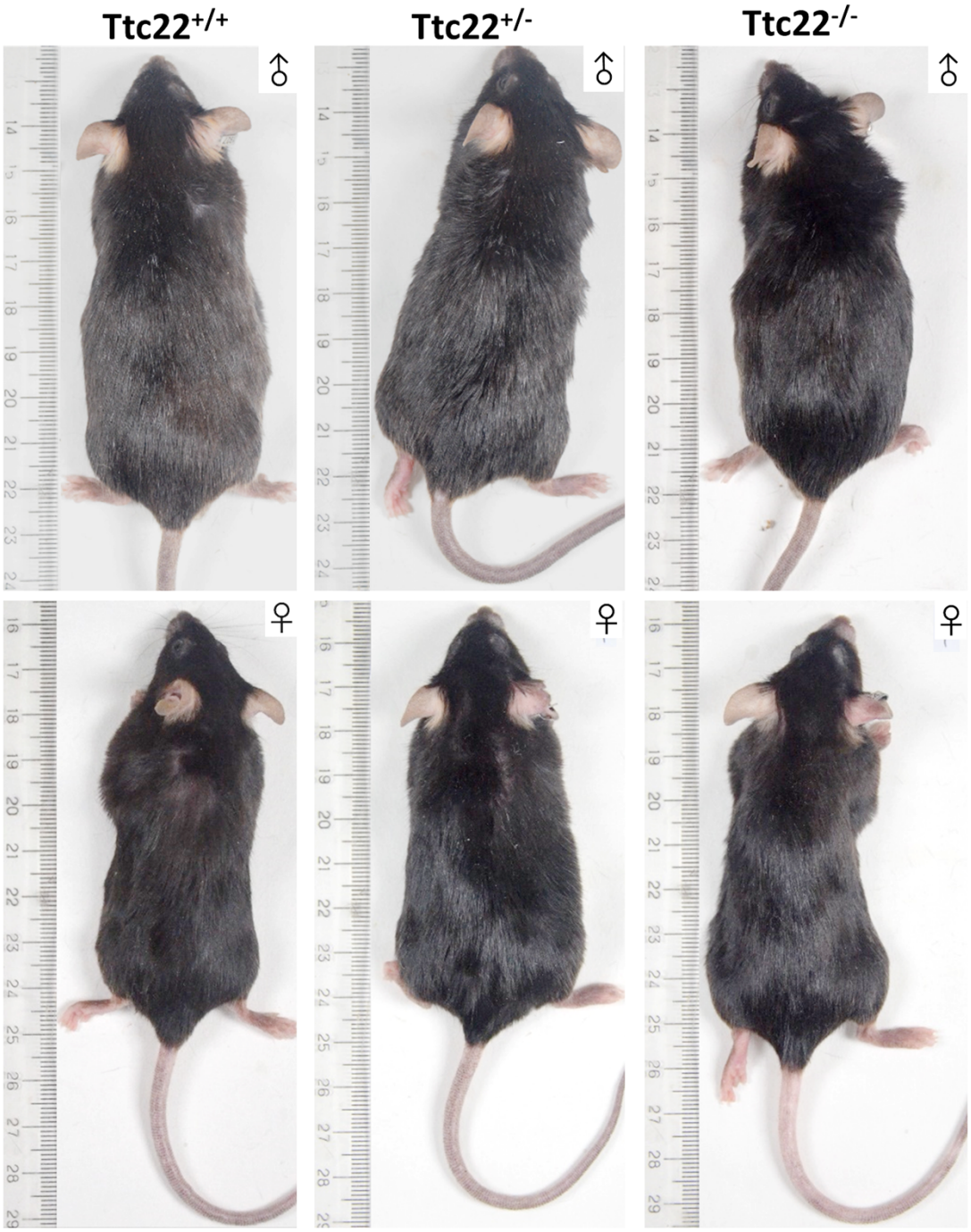

306

307 **Figure 2**. The appearance of C57BL/6N male and female C57BL/6N mice with different *Ttc22* genotypes at

308 approximately 66 and 77 weeks of age

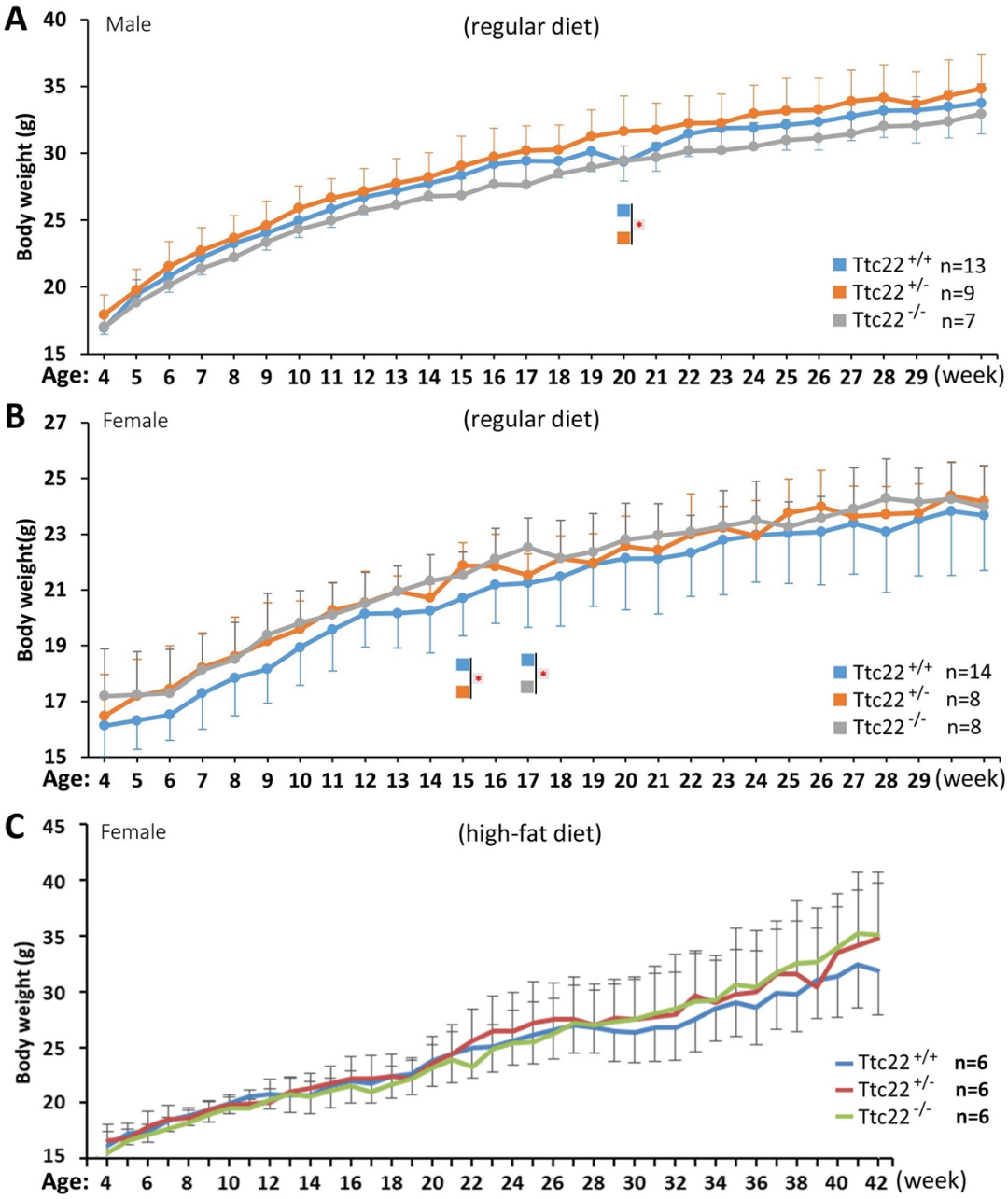

Figure 3. Body weight curves of C57BL/6N mice in different *Ttc22* genotype groups. (**A** and **B**) Body weight curves for male and female mice fed a regular diet. (**C**) Body weight curves for female mice fed a high-fat diet. The dots and bars represent the average and standard deviation (SD) of the body weights of the mice; *p<0.05 according to Student's t test.

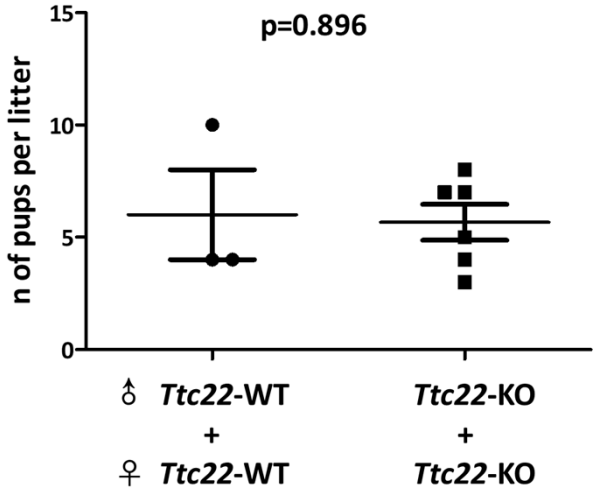

316

317 **Figure 4**. Fertility comparison between *Ttc22*$^{+/+}$ and *Ttc22*$^{-/-}$ mice.

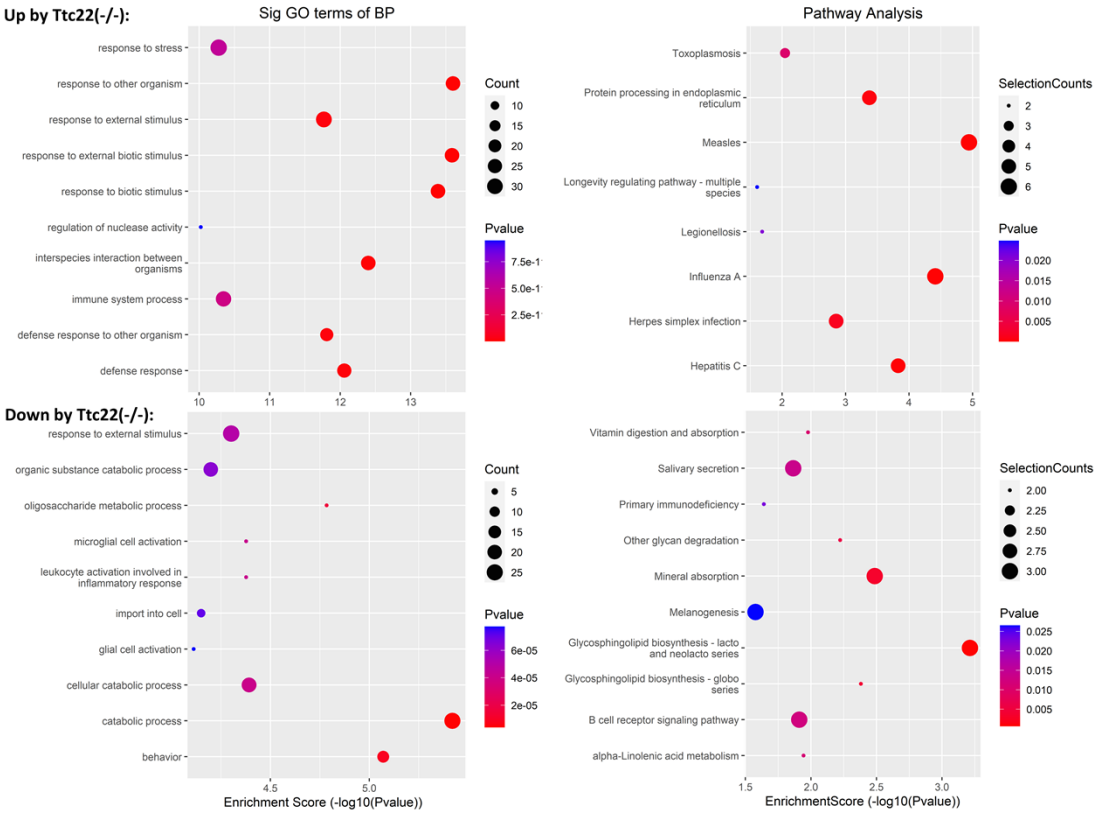

Figure 5. Enrichment scores for genes upregulated and downregulated by homozygous *Ttc22* knockout in the colon of 57-week-old male mice

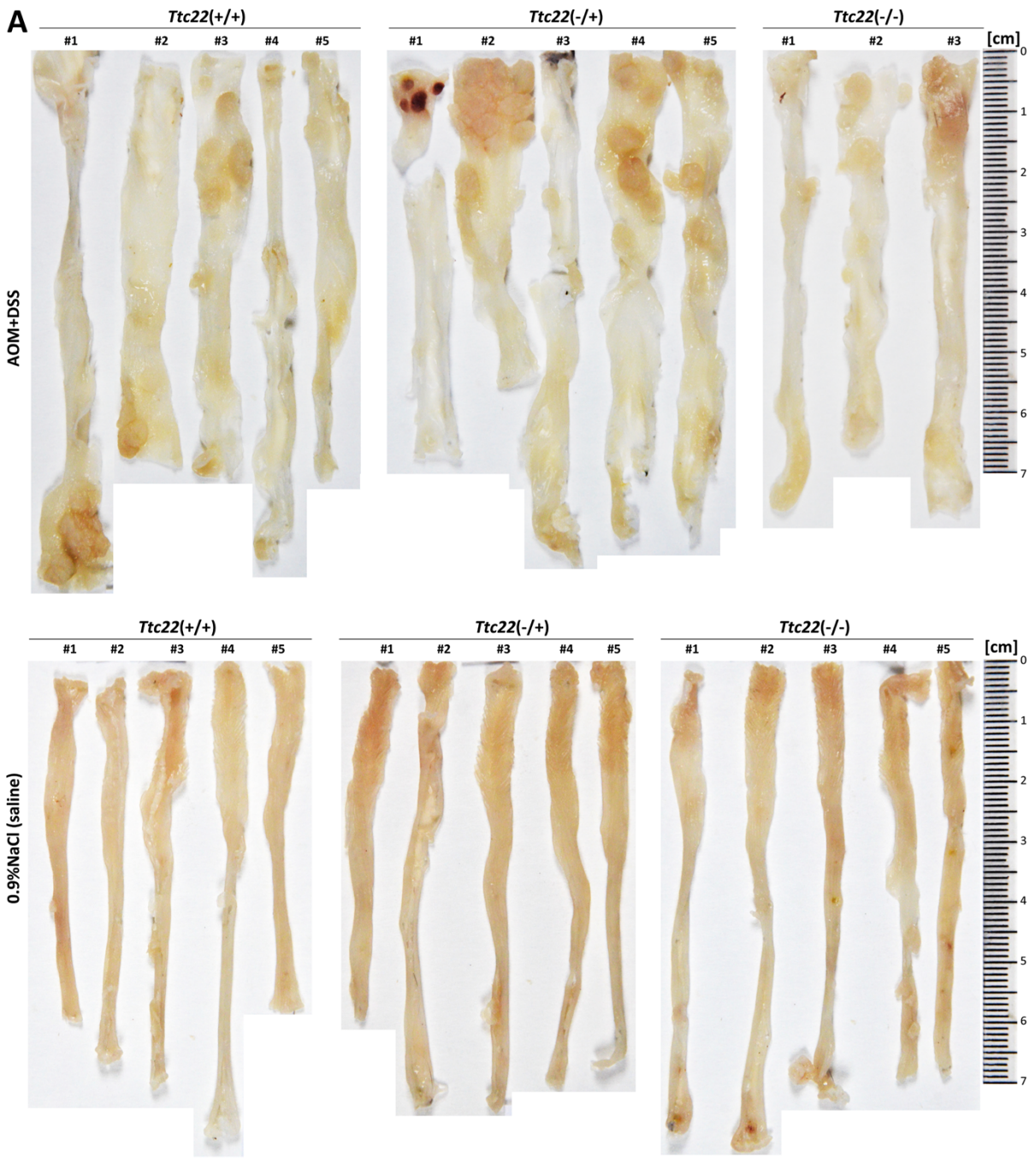

322

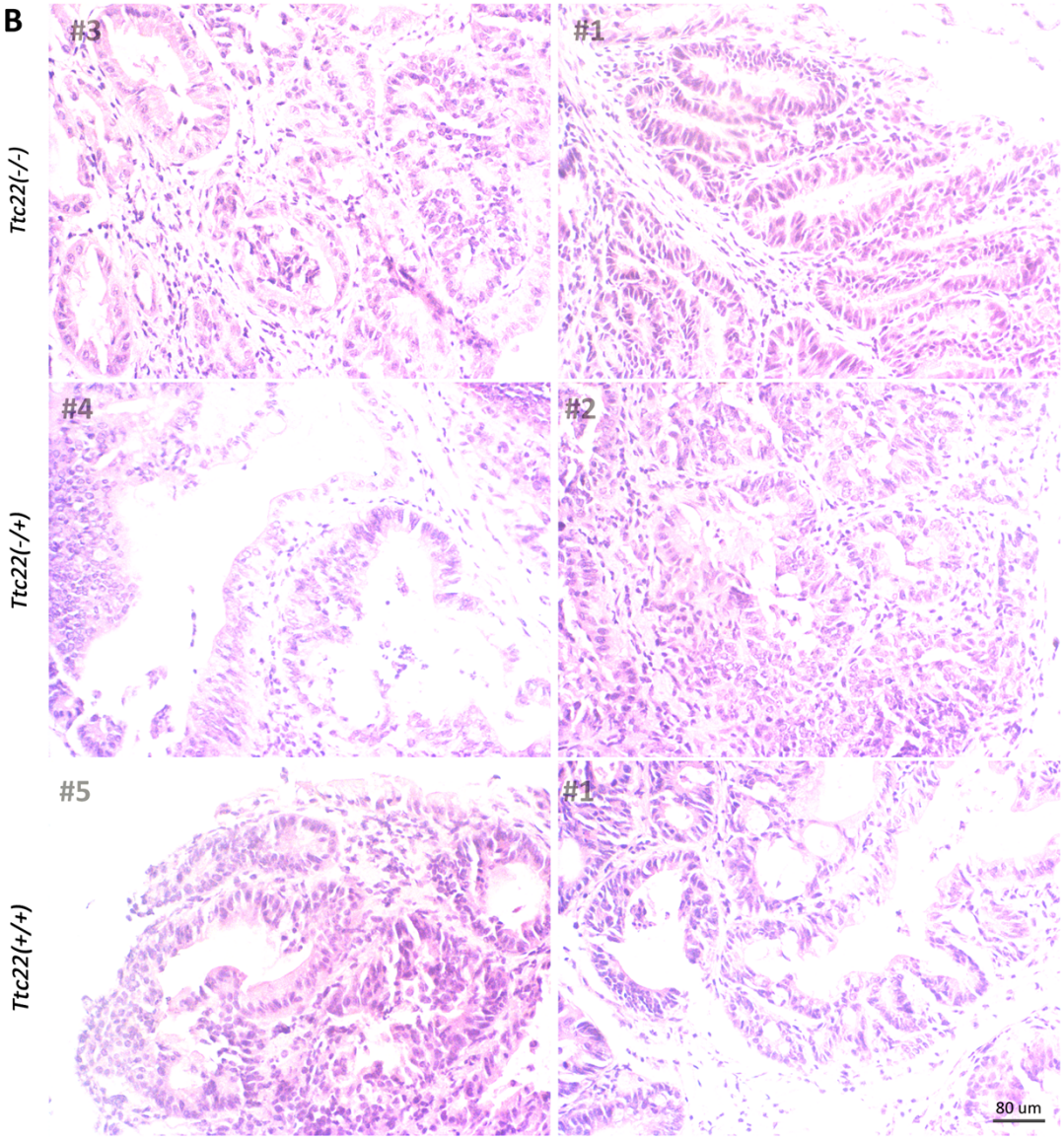

323

324 **Figure 6.** Induction of colon tumors by AOM/DSS in male C57BL mice with different *Ttc22* genotypes. (**A**) Overview

325 of tumors in the prefixed colon; (**B**) Histological images of representative tumors induced by AOM and DSS.

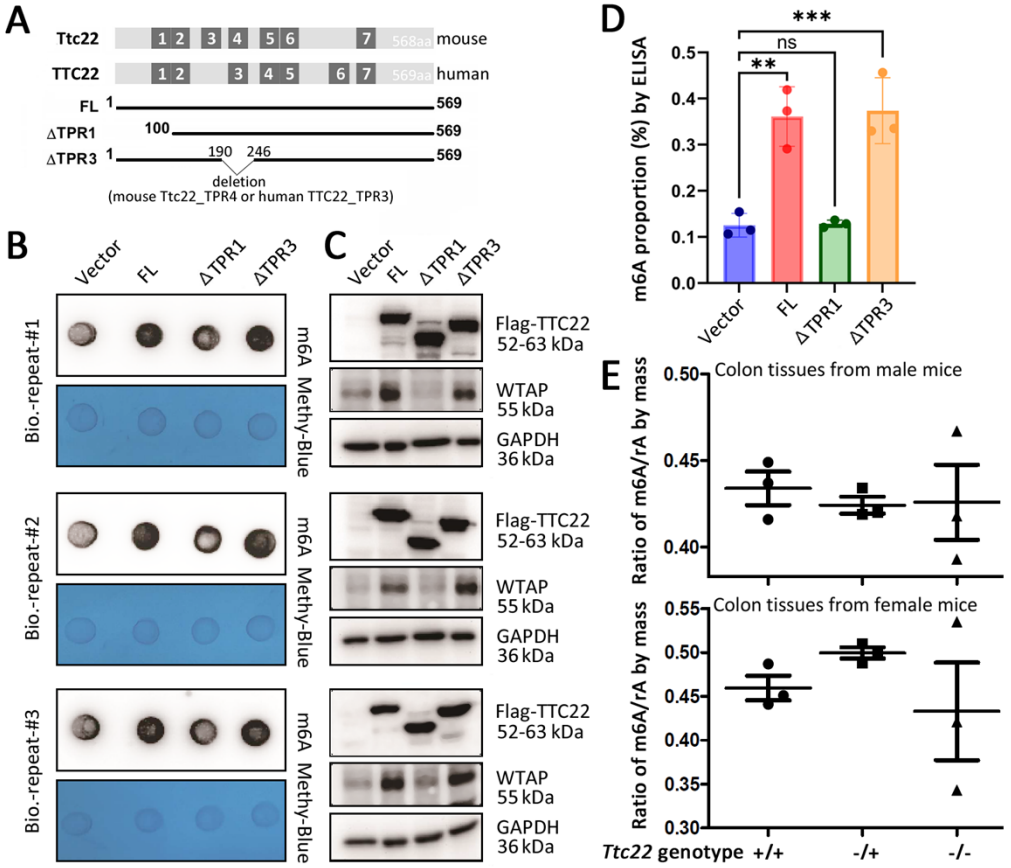

Figure 7. Effect of TTC22 TPR3 deletion on WTAP expression. (**A**) Illustration of various TTC22 variants, including the full-length TTC22 (FL) and its TPR1- or TPR3-deleted truncates (ΔTPR1 or ΔTPR3). (**B** and **C**) Effect of TTC22 TPR3 deletion on WTAP expression and total RNA m6A modification in HCT116 cells, as determined by Western blotting and m6A-specific dot blotting. (**D**) Effect of TTC22 TPR3 deletion on total RNA m6A modification in HCT116 cells, as determined by m6A-specific ELISA. (**E**) The ratio of total m6A to total adenosine in RNA (m6A/rA) in the colon tissues of mice with various *Ttc22* genotypes, as determined by mass.

335 ## TABLE LIST

336 **Table 1**. Incidence and latency period of spontaneous lymphoma in C57BL/6N mice with different *Ttc22* genotypes

Genotype	Male			Female		
	n	Mice with tumor (%)	Range of tumor latent weeks	n	Mice with tumor (%)	Range of tumor latent weeks
Ttc22$^{+/+}$	17	3 (17.6)	45, 55, 77	12	0	-
Ttc22$^{+/-}$	14	2 (14.3)	57, 60	19	4 (21.1)	57, 60, 65, 75
Ttc22$^{-/-}$	27	2 (7.4)	54, 54	39	6 (15.4)	41, 55, 55,55, 59, 60
(sum)	58	7 (12.1)		60	10 (16.7)	

337